Wiley Online Library
Early View publication on www.wileyonlinelibrary.com
(issue and page numbers not yet assigned;
citable using Digital Object Identifier – **DOI**)

Phys. Status Solidi A, 1600925 (2017) / **DOI** 10.1002/pssa.201600925

physica status solidi a
www.pss-a.com
applications and materials science

Extraction of net acceptor type trap density in semi-insulating GaN layers grown on Si substrate by DC *I–V* measurement

Taketoshi Tanaka*, Norikazu Ito, Minoru Akutsu, Kentaro Chikamatsu, Shinya Takado, and Ken Nakahara

Power Application Development Division, ROHM Co. Ltd., 21, Saiin Mizosaki-Cho, Ukyo-ku, Kyoto 615-8585, Japan

Received 6 December 2016, revised 21 March 2017, accepted 5 April 2017
Published online 26 April 2017

Keywords acceptor type traps, AlGaN/GaN HFETs, semi-insulating GaN, trap density

* Corresponding author: e-mail taketoshi.tanaka@dsn.rohm.co.jp, Phone: +81753216270, Fax: +81753111288

A simple quantitative method is proposed to estimate net acceptor-type trap density (N_T–N_D, where N_T denotes a gross acceptor-type trap density, and N_D denotes a donor density) in semi-insulating GaN layers, widely used as the electron channel layer in AlGaN/GaN heterojunction field-effect-transistors. The DC current–voltage characteristics of a semi-insulating GaN layer on a Si wafer have a threshold voltage (V_{TH}). Band diagram simulation reveals that N_T–N_D determines V_{TH}, and hence, the N_T–N_D in semi-insulating GaN films can be experimentally estimated by measuring V_{TH}.

1 Introduction The AlGaN/GaN heterojunction field-effect-transistor (HFET) has high potential in high frequency switching. This is due to the high electron mobility of the two-dimensional electron gas (2DEG) spontaneously generated by piezoelectric polarization in AlGaN/GaN combinations. For example, Kashiwagi et al. reported a 10-MHz switching of a recessed gate AlGaN/GaN HFET [1].

GaN layers in AlGaN/GaN HFETs, must possess semi-insulting properties to achieve low parasitic capacitance and cut off drain current during the off-state. Accordingly, the nitride films must incorporate a larger acceptor-type trap density (N_T) than the donor density (N_D) [2] to compensate themselves electrically, since GaN films, in general, unintentionally incorporate donors [3].

Assuming that N_D is fully ionized without an external bias, with $N_T > N_D$, the electrons occupy a part of N_T so that the density is equal to N_D, to maintain charge neutrality in GaN films. The unoccupied N_T remains under zero bias. These unoccupied traps, with a density of N_T–N_D, work as the net acceptor-type traps with the capability of capturing electrons. Accordingly, external biases change the charge state of GaN films from semi-insulating into negatively charged with a charge density of $q(N_T–N_D)$ where q is the elementary charge.

The N_T–N_D of semi-insulating GaN layers is an important parameter to determine the performance of AlGaN/GaN HFETs. A certain quantum of N_T–N_D reportedly plays an essential role to suppress the punch-though in short channel [4], and capture electrons, causing current collapse, which is a common problem with AlGaN/GaN HFETs [5]. Therefore, the N_T–N_D of semi-insulating GaN layers must be quantitatively estimated in order to simulate and control HFET's characteristics, and to monitor the epitaxial growth process of AlGaN/GaN structures in manufacturing.

However, the conventional methods to determine N_T are not satisfactory enough to estimate N_T–N_D in semi-insulating layers. Deep levels in GaN were studied using deep level transient spectroscopy (DLTS) [6, 7] and deep level optical spectroscopy (DOLS) [7, 8]. DLTS is useful for trap characteristics but difficult to investigate those of semi-insulating materials, because the semi-insulating materials are electrically fully depleted, leading to the external-bias insusceptibility of their measured capacitances [9, 10]. Moreover, DOLS does not measure N_D either, because all

donors in the semi-insulating materials are generally fully ionized due to the Fermi-level (E_F) pinned to deep levels [8].

While the fundamental and detailed physical properties of traps are always of scientific importance, this paper does not aim at to reveal such physics, but to focus on providing a design standard of epitaxial films for GaN based electronic devices. For this purpose, we propose a practical but quantitative measure to estimate N_T–N_D in semi-insulating crystalline GaN films.

Epitaxial GaN films were grown on high-conductive Si substrates, and electrodes were deposited on the GaN films and on the backside of the Si wafers. Current–voltage (I–V) curves of this structure clearly showed the threshold voltage (V_{TH}). Device simulation revealed that N_T–N_D in the GaN films defined V_{TH}. This means that N_T–N_D can be estimated by using the experimental values of V_{TH}, assuming that the electrons trapped in a deep level with a density of N_T–N_D are only the origin of the negatively charged state of an electrically biased semi-insulating film. Finally, we show that deep-level related photoluminescence correlates with the experimentally estimated N_T–N_D.

2 Simulation and experiments First, we qualitatively explain the reason for the appearance of V_{TH} for devices comprising GaN-on-Si sandwiched with metal electrodes.

Figure 1a–d show the band diagrams of a GaN film biased differently. Figure 1a exhibits the band diagram for no external bias, while the ones in Fig. 1b–d are for the right-side positively biased electrode formed on the backside of p-type Si, denoting "anode." For simplicity, we assume that the GaN incorporates only one trap level positioning at E_T (eV) above the valence band maximum, and that the trap captures all the electrons in the GaN with no external bias applied. These prerequisites lead to the E_F of the GaN being pinned to E_T.

Al, with a work-function (Φ_M) of 4.2 eV, is the contact electrode material. The E_F is positioned deeper than the Φ_M, making the energy band of the GaN bend downwards, near the semiconductor-contact interface. Accordingly, electrons occupy all trap sites near the contacts so as to make the E_F flat throughout the GaN, creating a built-in potential barrier at the interfaces, as shown in Fig. 1a.

In Fig. 1b, the anode has a small positive bias, and electrons begin to fill the trap sites, which were unoccupied under zero bias, thereby stopping the flow of electrons. Figure 1c exemplifies the situation of no unoccupied traps. When the system reaches this state, as there are no traps for the electrons to occupy, they begin to flow through the GaN, resulting in the appearance of V_{TH} in the I–V characteristics of the device. Larger positive bias finally nullifies the built-in potential, and the band monotonically bends downward, as represented in Fig. 1d. At this point, the GaN simply acts as a resistor.

Generally speaking, the validity of the above explanation probably depends on the transistion time of hole emission due to very few mobile electrons. However, approximately

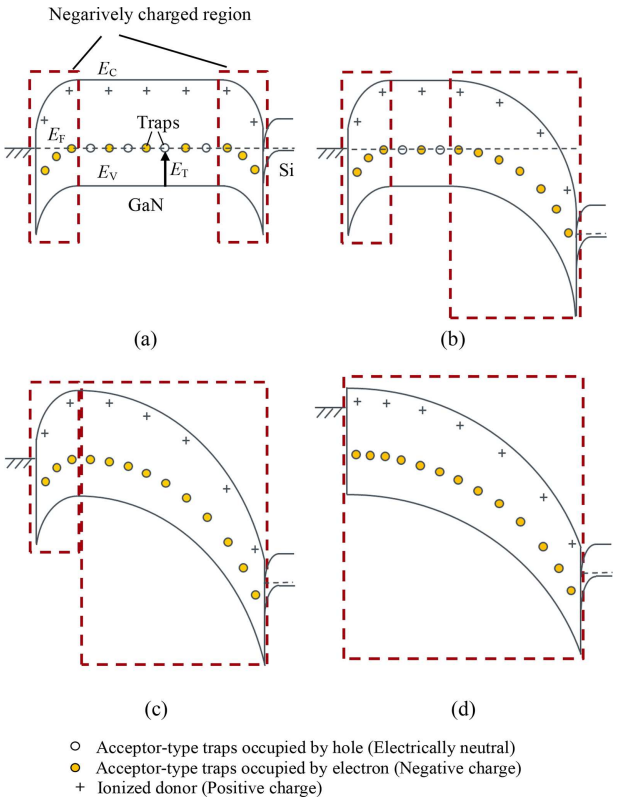

Figure 1 Band diagrams of the semi-insulating GaN film with (a) no external bias, (b) positively biased but below V_{TH}, (c) positively biased and above V_{TH}, (d) positively biased and above V_{TH}.

1 ms is enough to occupy all traps (Fig. 1d), if typical electron-capture cross-section is used ranging from 10^{-17} to $10^{-14}\,cm^{-2}$ [11–13]. Hence, deep traps can be detected by this N_T–N_D estimation method, if we use DC I–V measurement

The authors use Sentaurus Device of Synopsys Incorporated, as the simulator device to carry out one-dimensional simulation in order to obtain the quantitative picture of the band diagrams, shown in Fig. 1, and the I–V characteristics for a 1.5 μm semi-insulating GaN on p-type Si sandwiched with electrodes. Since the background carrier density reportedly ranges from 10^{15} to $10^{17}\,cm^{-3}$ for GaN [14–16], we set the level of N_D at an average value of $1\times10^{16}\,cm^{-3}$ in the GaN film. N_T of $5\times10^{16}\,cm^{-3}$ is introduced for reproducing semi-insulating behavior of the GaN. E_T is set in the GaN to be 0.9 eV above the valence band maximum edge (E_V), because carbon is often claimed as a major candidate for acceptor-type traps [17].

Figure 2a depicts the simulation results showing the bending of conduction band minimum edge (E_C) with applied bias, with the anode on the right-side, and the cathode on the left-side. Figure 2b shows the simulated I–V curve. Annotations (A)–(D) in Fig. 2a and b are used to identify the bias states of the band diagrams and of the I–V situation. As described in detail afterwards, two kinds of V_{TH} appear below. One is the $V_{TH}^{(s)}$ given by simulated I–V curves, and $V_{TH}^{(m)}$ is given by the measured I–V data.

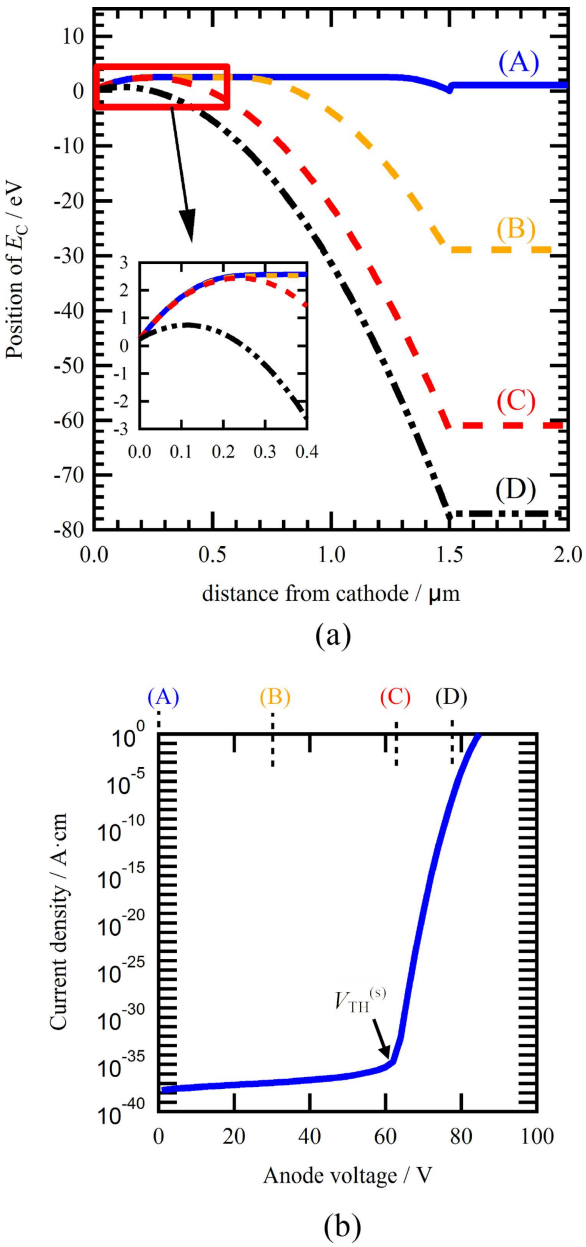

Figure 2 (a) E_C bending with various bias situations. The inset magnifies the E_C bending around the cathode, (b) Simulated *I–V* characteristics.

The E_C, denoted by (A)–(D) in Fig. 2a, in principle, correspond to the band diagrams shown in Fig. 1a–d, respectively. Similarly, the E_C bending is as shown in Fig. 1, and the built-in potential at the semiconductor-electrode interface almost disappears at (D)-state, as shown in the inset figure. Figure 2b depicts $V_{TH}^{(s)}$ corresponding to (C)-state. At voltages below $V_{TH}^{(s)}$, which corresponds to (A) to (B)-states, the built-in potential does not significantly change, as shown in the inset of Fig. 2a. The built-in potential starts diminishing when the external bias goes above $V_{TH}^{(s)}$ in (D)-state, and consequently, the current increases exponentially.

It should be noted, however, that the $V_{TH}^{(s)}$ does not coincide with $V_{TH}^{(m)}$, since the $V_{TH}^{(s)}$ value is too small for measurement. The current density below $\sim 10^{-10}\,A\cdot cm^{-2}$ is low and off-scale for a typical *I–V* analyzer. As shown in Fig. 2b, a current density of $10^{-10}\,A\cdot cm^{-2}$ is realized in (D)-state. Therefore, the experimentally observed V_{TH} is denoted as $V_{TH}^{(m)}$ here to distinguish from $V_{TH}^{(s)}$. At $V_{TH}^{(m)}$, the band diagram is (D), and the electrons fully occupy the trap sites in the GaN, resulting in the film being negatively charged with $q(N_T–N_D)\ C\cdot cm^{-3}$, where q is the elemental charge, and the total unoccupied trap density is $N_T–N_D$. Since these charges are uniformly distributed in the GaN, the Poisson's equation provides $N_T–N_D$ as

$$N_T - N_D = \frac{2\varepsilon_0 \varepsilon V_{TH}^{(m)}}{qd^2}, \quad (1)$$

where d denotes the thickness of the GaN layer, ε is the relative dielectric constant of GaN, and ε_0 is the permittivity of vacuum. This equation experimentally determines $N_T–N_D$.

The experiment preparations are described in this paragraph. All nitride films were grown by metal organic chemical vapor deposition. An intentionally un-doped 0.1-μm AlGaN/0.2-μm AlN structure was used as a buffer for semi-insulating GaN growth on highly conductive (1–4 mΩ·cm) p-type Si (111) substrates. The buffer prevents Si from melt-back etching caused by Ga [18]. Ti/Al (Ti followed by Al) cathode and anode electrodes were formed on the surface of the nitride layers and on the backside of the Si wafers, respectively. Since the extra charges expected for $N_T–N_D$ of GaN should appear in the buffer layer and in each interface such as poralization charges, we prepared two different kinds of structures to experimentally determine the $N_T–N_D$ of semi-insulating GaN films. Sample-A included 0.1-μm GaN/0.1-μm AlGaN/0.2-μm AlN template, whereas, Sample-B had a 1.4-μm GaN layer subsequently grown on the template of Sample-A. External voltages did not change the capacitance value of these samples, which was based on the total thickness. This establishes that the nitride layers were semi-insulating.

The anodes are positively biased for samples A and B, and the *I–V* analyzer (B1505A of Agilent Technologies) is used to obtain the *I–V* curves of the samples as shown in Fig. 3. The *I–V* curves exhibit $V_{TH}^{(m)}$, as expected by the simulated results. Assuming no significant difference in dielectric constants between AlN and AlGaN, the difference of $V_{TH}^{(m)}$, between Sample-A and Sample-B (ΔV_{TH}) is determined by the $q(N_T–N_D)/\varepsilon_0\varepsilon$ of the GaN. The calculation process is explained in Fig. 4. Hence, $N_T–N_D$ of the GaN is given by

$$N_T - N_D = \frac{2\varepsilon_0 \varepsilon \Delta V_{TH}}{q(2d_{GaN}d_{template} + d_{GaN}{}^2)}, \quad (2)$$

where d denotes the film thickness, and the subscripts of GaN and template are used to show the values for added GaN layer

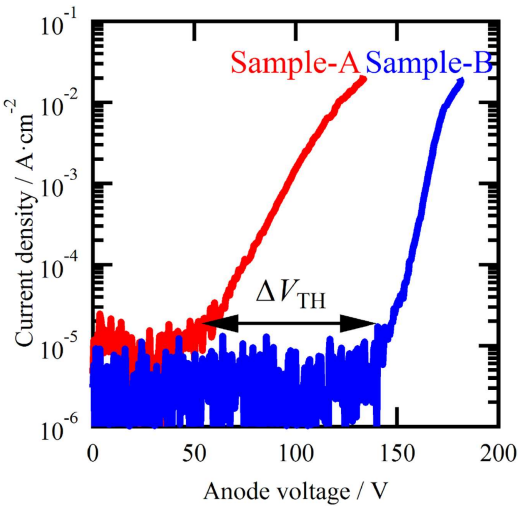

Figure 3 *I–V* characteristics of experimental samples.

of Sample-B and GaN/AlGaN/AlN template, respectively. This equation determines the N_T–N_D of the GaN layer in Sample-B to be $2.8 \times 10^{16}\,cm^{-3}$. This value of N_T–N_D coincides with the reported trap density which ranges from 10^{15} to 10^{17} as measured by DLTS and DOLS [6–8].

Photoluminescence (PL) measurement excited by a He-Cd laser was also performed, to show the appropriateness of the method proposed here, to estimate N_T–N_D. Three pairs of samples are prepared, and each pair has the same device structure as that of Sample-A and Sample-B. The GaN films therein are grown at a temperature (T_g) of 1080, 1110, and 1140 °C in order to vary the carbon concentration [19]. The use of these different T_g provides a carbon concentration of 1.2×10^{18}, 9.0×10^{17}, and $8.3 \times 10^{16}\,cm^{-3}$, respectively, confirmed by a secondary ion mass spectroscopy. The ΔV_{TH} is measured by comparing $V_{TH}^{(m)}$ of sample-A and −B structure device of each pair, and thus, the N_T–N_D is determined by Eq. (2).

The sample-B structure devices are used for PL measurements. The PL specta peak at the photon energy of approximately 2.2 and 2.9 eV, namely yellow luminescence

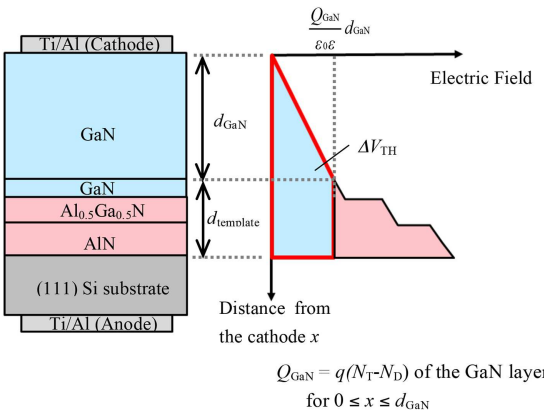

Figure 4 Schematic of structure and electric field of Sample-B.

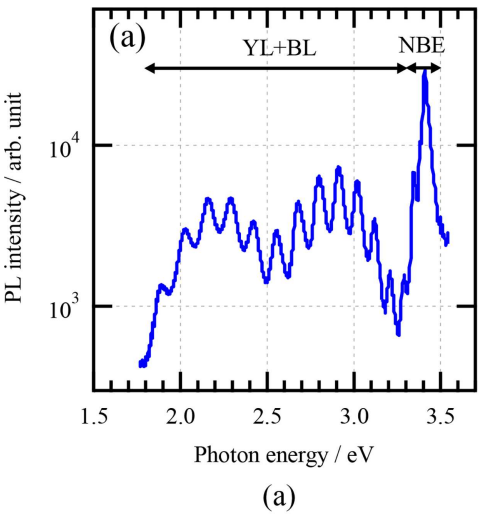

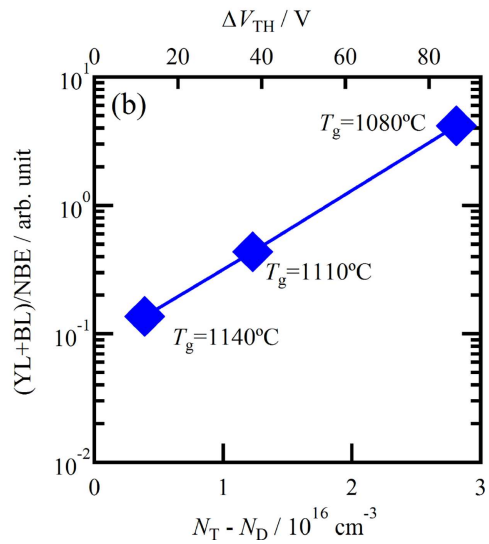

Figure 5 (a) A PL spectrum of a semi-insulating GaN film of Sample-B grown at $T_g = 1080\,°C$. (b) Correlation between (YL + BL)/NBL and the N_T–N_D calculated by Eq. (2).

(YL) and blue luminescence (BL), are observed as shown in Fig. 5a. These peaks reportedly relate to deep levels in GaN [17, 20, 21].

Figure 5b shows the correlation of N_T–N_D with the PL strength ratio defined by (YL + BL)/NcBE, where YL + BL and NBE denote the PL strength integrated over the photon energy range of 1.8–3.3 eV and of 3.3–3.5 eV, respectively. The linear correlation of $\log_{10}$[(YL + BL)/NBE] to N_T–N_D are clearly seen, and this fact upholds the proposed method to estimate N_T–N_D.

3 Conclusions Band diagram simulation for a semi-insulating GaN film sandwiched electrode reveals that the *I–V* curve of the structure has V_{TH} determined by N_T–N_D, including the semi-insulating semiconductor. Experimental *I–V* curves coincide well with the simulated counterparts, and therefore, the $V_{TH}^{(m)}$ provides a simple and useful

quantitative measure to determine N_T–N_D. N_T–N_D values determined by using $V_{TH}^{(m)}$, linearly correlate to $\log_{10}$[(YL + BL)/NBE], which quantitatively show the appropriateness of our proposed method to estimate N_T–N_D.

References

[1] J. Kashiwagi, T. Fufiwara, M. Akutsu, N. Ito, K. Chikamatsu, and K. Nakahara, IEEE Electron. Device Lett. **34**, 1109, (2013).
[2] G. Verzellesi, L. Morassi, G. Meneghesso, M. Meneghini, E. Zanoni, G. Pozzovivo, S. Lavanga, T. Detzel, O. Häverlen, and G. Curatola, IEEE Electron. Device Lett. **35**, 443 (2014).
[3] G. Y. Zhang, Y. Z. Tong, Z. J. Yang, S. X. Jin, J. Li, and Z. Z. Gan, Appl. Phys. Lett. **71**, 3376 (1997)
[4] M. J. Uren, K. J. Nash, R. S. Balmer, T. Martin, E. Morvan, N. Caillas, S. L. Delage, D. Ducatteau, B. Grimbert, and J. C. De Jaeger, IEEE Trans. Electron. Devices **53**, 395 (2006).
[5] Y. Ohno, Y. Kio, and J. P. Ao, Jpn. J. Appl. Phys. **52**, 08JN28 (2013).
[6] W. J. Wang, C. L. Liao, Y. F. Chang, Y. L. Lee, C. L. Ho, and M. C. Wu, IEEE Electron. Device Lett. **34**, 1376 (2013).
[7] Z. Zhang, C. A. Hurni, A. R. Arehart, J. Yang, R. C. Myers, J. S. Speck, and S. A. Ringel, Appl. Phys. Lett. **100**, 052114 (2012)
[8] A. Armstrong, C. Poblenz, D. S. Green, U. K. Mishra, J. S. Speck, and S. A. Ringel, Appl. Phys. Lett. **88**, 082114 (2006).
[9] H. Matsuura, Y. Kagawa, M. Takahashi, S. Tano, and T. Miyake, Jpn. J. Appl. Phys. **48**, 056504 (2009).
[10] W. C. Mitchel, William D. Mitchell, H. E. Smith, G. Landis, S. R. Smith, and E. R. Glaser, J. Appl. Phys. **101**, 053716 (2007).
[11] Z-Q. Fang, D. C. Look, W. Kim, Z. Fan, A. Botchkarev, and H. Morkoç, Appl. Phys. Lett. **72**, 2277 (1998).
[12] S. D. Brotherton and J. Bicknell, Appl. Phys. Lett. **49**, 667 (1978).
[13] Marco Silvestri, Michael J. Uren, and Martin Kuball, Appl. Phys. Lett. **102**, 073501 (2013).
[14] J. A. Freitas, Jr., M. A. Mastro, E. A. Imhoff, M. J. Tadjer, C. R. Eddy, Jr., and F. J. Kub, J. Cryst. Growth **312**, 2616 (2010).
[15] V. Bousquet, J. Heffernan, J. Barnes, and S. Hooper, Appl. Phys. Lett. **78**, 754 (2001).
[16] N. H. Karam, T. Parodos, P. Colter, D. McNulty, W. Rowland, J. Schetzina, N. El-Masry, and S. M. Bedair, Appl. Phys. Lett. **67**, 94 (1995).
[17] J. L. Lyons, A. Janotti, and C. G. Van de Walle, J. Appl. Phys. **97**, 152108 (2010).
[18] H. Ishikawa, G. Y. Zhao, N. Nakada, T. Egawa, T. Soga, T. Jimbo, and M. Umeno, Phys. Status Solidi A **176**, 599 (1999).
[19] D. D. Koleske, A. E. Wickenden, R. L. Henry, and M. E. Twigg, J. Cryst. Growth **242**, 55 (2002).
[20] M. A. Reshchikov, F. Shahedipour, R. Y. Korotkov, B. W. Wessels, and M. P. Ulmer, J. Appl. Phys. **87**, 3351 (2000).
[21] M. A. Reshchikov and H. Morkoç, J. Appl. Phys. **97**, 061301 (2005).